Master Thesis

Signal and background studies for scalar leptoquark pair production in the $\mathbf{t\bar{t}+2\tau}$ channel at the ATLAS experiment

Daniel Adlkofer

Supervisor
Prof. Dr. Raimund Ströhmer

Advisor
Dr. Mahsana Haleem

November 2018

Physikalisches Institut
Lehrstuhl für Physik und ihre Didaktik
Julius-Maximilians-Universität Würzburg

Contents

1

XyZ

2 eV m^{-1}

sample	$\mathbf{t\bar{t}}$		$\mathbf{t\bar{t}H}$	
selection	reconstruction event yield	truth event yield	reconstruction event yield	truth event yield
≥ 2 b-jets	66878	252200	73	200
≥ 2 b-jets $+1\,\tau$	188	5923	2.5	28
≥ 2 b-jets $+2\,\tau$	0.7	49	0.2	8.2

Table 1.1: Event yield for different selections with tau leptons for the $t\bar{t}$ and the $t\bar{t}H$ Monte Carlo sample. The luminosity account for 36.1 fb^{-1}.

sample	$\mathbf{t\bar{t}}$	$\mathbf{t\bar{t}H}$
selection	efficiency $\frac{\epsilon}{\%}$	efficiency $\frac{\epsilon}{\%}$
≥ 2 b-jets	26.52	36.72
≥ 2 b-jets $+1\,\tau$	3.18	8.83
≥ 2 b-jets $+2\,\tau$	1.41	2.13

Table 1.2: Efficiencies for different selections with tau leptons for the $t\bar{t}$ and the $t\bar{t}H$ Monte Carlo sample.

sample		**$t\bar{t}$**		**$t\bar{t}H$**	
selection	reference selection	reconstruction ratio $\frac{r}{\%}$	truth ratio $\frac{r}{\%}$	reconstruction ratio $\frac{r}{\%}$	truth ratio $\frac{r}{\%}$
≥ 2 b-jets $+1\,\tau$	≥ 2 b-jets	0.28	2.35	3.43	14.26
≥ 2 b-jets $+2\,\tau$	≥ 2 b-jets	0.0011	0.020	0.24	4.11

Table 1.3: Ratios for different selections with tau leptons for the $t\bar{t}$ and the $t\bar{t}H$ Monte Carlo sample.

sample	**$t\bar{t}$**		**$t\bar{t}H$**	
selection	numerator event yield	denominator event yield	numerator event yield	denominator event yield
truth matching for tau	63	13723	5590	21610
efficiency	0.46%		25.9%	
tau from H^0, $W^{\pm}$, Z^0	0	0	4859	11988
efficiency	-		40.5%	
tau from B-mesons	63	13722	20	7416
efficiency	0.46%		0.27%	
tau within a jet	8440	3776952	18511	20327225
efficiency	0.22%		0.091%	
tau within a b-jet	6098	2658379	2317	1208924
efficiency	0.23%		0.19%	

Table 1.4: Event yield for different selections with tau leptons for the $t\bar{t}$ and the $t\bar{t}H$ Monte Carlo sample. The luminosity account for $36.1\,\mathrm{fb}^{-1}$.

sample	$LQ_{500\,GeV}$		$LQ_{1\,TeV}$	
selection	numerator event yield	denominator event yield	numerator event yield	denominator event yield
truth matching for tau	2604	5362	2263	5055
efficiency	48.6%		44.8%	
tau from H^0, $W^\pm$, Z^0	95	340	82	461
efficiency	27.9%		17.8%	
tau from B-mesons	0	183	0	200
efficiency	0.0%		0.0%	
tau from LQ	1744	3286	1057	2022
efficiency	53.1%		52.3%	
tau within a jet	7232	55208	7011	63671
efficiency	13.1%		11.0%	
tau within a b-jet	2317	1208924	6098	2658379
efficiency	0.45%		0.23%	

Table 1.5

2

Introduction

3

Theoretical background for the search of scalar leptoquarks

3.1 The Standard Model of particle physics

4

Experimental setup for the search of scalar leptoquarks

For the search of scalar leptoquarks the ATLAS detector at the Large Hadron Collider (LHC) is used as experimental setup which will be described within this chapter. In section 4.1 the general setting of the proton-proton collider located at the CERN research center is the subject of interest. The particle detection of the resulting collision events will take place in the ATLAS detector with its different specialized components (section 4.2). Section 4.3 addresses the leptoquark pair production in proton-proton collisions.

4.1 The Large Hadron Collider accelerator complex

The research center CERN (Conseil Européen pour la Recherche Nucléaire) was founded in 1954 near Geneva, Switzerland to become a major European joint venture on elementary particle physics. In the mean time 22 member states are participating in that large-scale project with the ambition to probe the essential constitutes of nature and the fundamental forces acting between them. [1]

In the huge accelerator complex protons reach through different stages energies of 6.5 TeV and will be brought to collisions at defined interaction sites in time intervals of 25 ns. Particle detectors then register signatures of the resulting collsion events and the analysis of new created particles gives insight to the nature of elementary particle physics.
Figure 4.1 shows the different acceleration stages. Starting from the injection protons will gain as much energy as 50 MeV in the linear accelerator LINAC2 and will

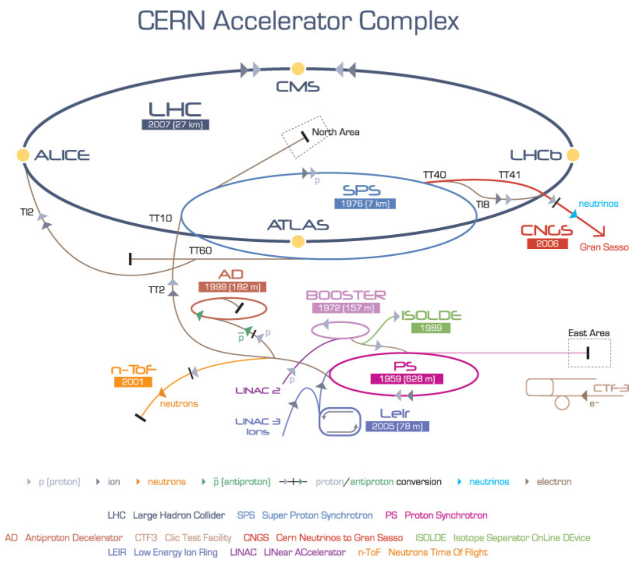

Figure 4.1: Schematic of the CERN accelerator complex with its different stages and few experiments like ATLAS located at a crossing point for protons. [2]

be further transferred to the Proton Synchrotron Booster (1.4 GeV), the Proton Synchrotron (25 GeV), the Super Proton Synchrotron (450 GeV) and finally to the LHC ring with its 26.7 km circumference. [1]
The LHC is designed as two-ring proton-proton collider. Conditions for a stable proton beam are diversely including high vacua of 10^{-10} mbar to 10^{-11} mbar and temperatures of 1.9 K for the superconducting NbTi-magnets of the accelerator. [3]

Different more experiments like ALICE[4], LHCb[5] are located at CERN due to the variety of research questions. But the subject of interest in this work lies in the high luminosity experiment ATLAS specialized for proton-proton collisions like its counterpart CMS[6].

4.2 The ATLAS detector at the LHC

One of the general purpose detector for proton-proton collisions is the ATLAS detector. This 25 m tall detector is located at one interaction point of the LHC where bunches, consisting of approximately 10^{11} protons, collide at a rate of 40 MHz [7]. The number of particles encountered per time is given by [8]

$$\dot{N} = \mathcal{L}\sigma \tag{4.1}$$

with the cross section σ for the present event and the instant luminosity $\mathcal{L}$. Given a measure for the number of collisions per unit time the instant luminosity can be introduced and is often used as key parameter in collider physics [3].

$$\mathcal{L} = \frac{N_b n_b f_{\text{rev}} \gamma_r}{4\pi\epsilon_n \beta^*} F \tag{4.2}$$

Where N_b is the number of particles per bunch, n_b the number of bunches per beam, f_{rev} the rotational frequency, γ_r the Lorentz factor, ϵ_n the normalized transverse beam emittance, β^* the betatron function at the collision point and F respects the geometric luminosity reduction factor due to the crossing angle at the collision point. The design luminosity for ATLAS was exceeded with $\mathcal{L} = 2.05 \times 10^{34}\,\text{cm}^{-2}\,\text{s}^{-1}$ for 2.05 times on the 2^{nd} of November 2017 emphasizing the great success over the years [9].

The aspiration to be sensitive to the great variety of particles governed by the fundamental forces (see chapter 3.1) influenced the detector design accordingly. The layered structure reflects the fact that The basic structure of ATLAS is shown in figure 4.2 with its different sub-detector systems together with the convention for the used coordinate system. The nominal interaction point acts as origin of the coordinate system where the z-axis follows the beam line. Perpendicular to the z axis lies the transverse x-y-plane usually described through the azimuthal angle ϕ. The positive x-axis points towards the center of the LHC. The cylindric symmetry of the detector suggests a cylindric coordinate system with the angle θ starting from the beamline. [7] Since the polar angle is not a Lorentz invariant quantity it is useful to describe the position in terms of rapidity $w = \frac{1}{2} \ln \frac{E+p_z c}{E-p_z c}$ in that highly relativistic regime. In the limit of massless particles the rapidity can be formulated as pseudorapidity $\eta = -\ln \tan \frac{\theta}{2}$.

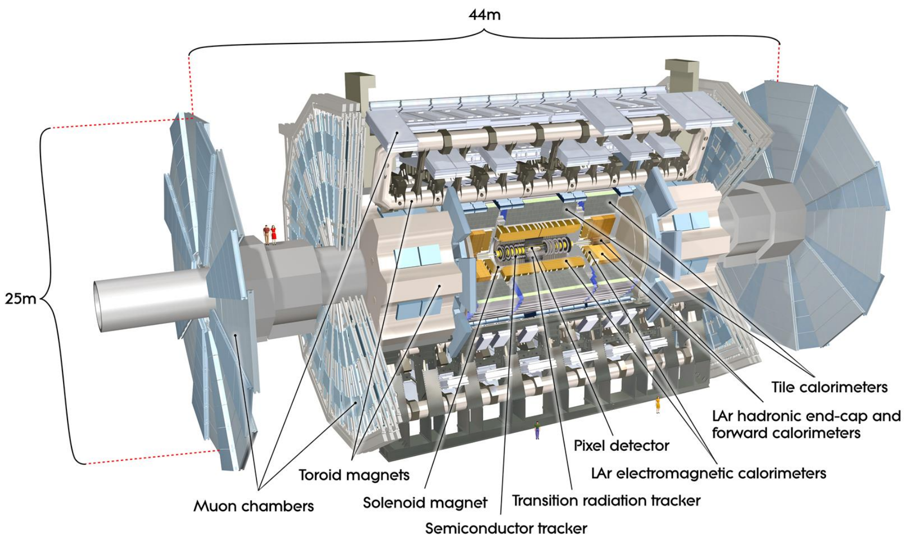

Figure 4.2: The layered structure of the ATLAS detector at the LHC and the used cylindric coordinate system. [7]

The magnet configuration includes a superconducting selenoid with a field strength of 2 T sourrounding the inner detector as well as three large superconducting toroid magnets around the calorimeter.
The inner detector is responsible for pattern recognition, momentum and vertex measurements and electron identification which is achieved with a combination of semiconductor pixel and strip detectors. Additional straw tube tracking detectors are sensitive to transistion radiation in the outer part.
Liquid argon electromagnetic sampling **calorimeter** with high granularity allow an excellent energy performance. It covers the range $|\eta| < 3.2$. For hadronic energy measurements a scintillator-tile calorimeter covering $|\eta| < 1.7$ is in operation. Further LAr technology is used for hadronic particles in the outer pseudorapidity range of $|\eta| > 1.5$. The forward calorimeters extend the coverage for hadronic and electromagnetic energy measurements to $|\eta| = 4.9$.
The **muon system** is suited in the outer layer of ATLAS and provides as independent system resolution for high energy muon tracks with three layered precision chambers. This is possible because of the air-cored toroid magnet system including one barrel and two end-cap magnets generating strong bending power in a large volume.

The data recording rate is limited due to technology and resource limitations and has to be reduced from 40 MHz to 200 MHz. This poses high demands on the **trigger system** which is organised in three levels. Level 1 uses only a subset of the total detector information making basic decisions to flag so called regions of interest. The output rate after this first selection accounts for 75 kHz. The high level trigger 2 and 3 are responsible for data reduction down to the final data-taking rate of 200 Hz writing events of the size of approximately 1.3 MB. [7]

4.3 Leptoquark pair production in proton-proton collisions

List of Figures

List of Tables

Bibliography

[1] CERN. About CERN. https://home.cern/about. visited on 4^{th} September 2018.

[2] CERN. Cern komplex. http://www.lhc-facts.ch/img/news2015/lhccomplex_.jpg. Last update: October 29, 2011.

[3] Lyndon Evans and Philip Bryant. Lhc machine. *Journal of Instrumentation*, 3(08):S08001, 2008.

[4] The ALICE Collaboration, K Aamodt, et al. The alice experiment at the cern lhc. *Journal of Instrumentation*, 3(08):S08002, 2008.

[5] The LHCb Collaboration, A Augusto Alves Jr, et al. The lhcb detector at the lhc. *Journal of Instrumentation*, 3(08):S08005, 2008.

[6] The CMS Collaboration, S Chatrchyan, et al. The cms experiment at the cern lhc. *Journal of Instrumentation*, 3(08):S08004, 2008.

[7] The ATLAS Collaboration, G Aad, et al. The atlas experiment at the cern large hadron collider. *Journal of Instrumentation*, 3(08):S08003, 2008.

[8] Donald H. Perkins. *Introduction to High Energy Physics -*. Cambridge University Press, Cambridge, 4. aufl. edition, 2000.

[9] Rende Steerenberg. Lhc report: Lhc reaches 2017 targets. https://home.cern/cern-people/updates/2017/11/lhc-report-lhc-reaches-2017-targets. posted by Stefania Pandolfi on 7 Nov 2017. Last updated 26 Jun 2018, 17.32.